社団法人　情報処理学会　研究報告
IPSJ SIG Technical Reports

2005－ＡＶＭ－51（４）
2005／12／12

双方向伝送技術を適用したマルチファイバ型 WDM リング網構成法

小原　仁　　坂田　真人

秋田大学　工学資源学部　電気電子工学科　〒010-8502 秋田市手形学園町 1-1

Performance analysis of bidirectional multifiber WDM express networks for metro areas

Hitoshi OBARA and Masato SAKATA

The EEE Department of AKITA University, 1-1 Tegata Gaken, Akita, 010-8502 Japan

E-mail: obara@ee.akita-u.ac.jp

Abstract　A design of multifiber WDM express networks of ring topology using two identical sets of wavelengths for opposite directions on a single fiber in a disjoint manner is introduced.

Keywords　Optical networks,　WDM,　Ring networks,　Bidirectional transmission, Multifiber

1. Introduction

This paper focuses on architectural designs of metro backbone networks shown in Fig. 1, where WDM ring networks are employed in both core network and satellite networks. Optical add/drop multiplexers (OADM's) are widely used in the WDM ring networks. Hub-and-satellite rings shown in Fig. 2 are used in the access rings, and OADM's provide wavelength channels between hub and sattelite nodes.

We consider a design of the core ring in Fig. 1, where its traffic volume far exceeds the capacity of a single WDM fiber, and thus multiple fibers are required. Some people may use multiple WDM transmission systems in parallel between two adjacent nodes and ultra high-capacity routers in every node, although they know such a primitive design is very expensive due to OEO conversion and inflated router capacity needed at every node. Some cost-aware people will prefer a stack of multiple WDM ring networks, one of which is shown in Fig. 2. However, they also find that many OADM's are necessary in every node. As a consequence, we see that no conventional design principle provides a cost-effective solution for high-capacity metro WDM core networks.

We believe that the multifiber WDM express networks (MWEN's) offer a new solution for such applications, because MWEN's need simple and economic OADM's as described later. However, MWEN's require a more number of fibers than that of those two designs described above. In this paper, we show that bidirectional transmission techniques can halve the number of fibers. Our design does not use WDM interleaver as conventional bidirectional transmission techniques. Instead, we use two identical sets of wavelengths for opposite directions on a single fiber in a disjoint manner. Bidirectional transmission using a pair of replicated wavelengths has never been thought to be feasible due to Rayleigh backscattering (RB) noise, because beat interference noise from RB causes a severe degradation of transmission quality.

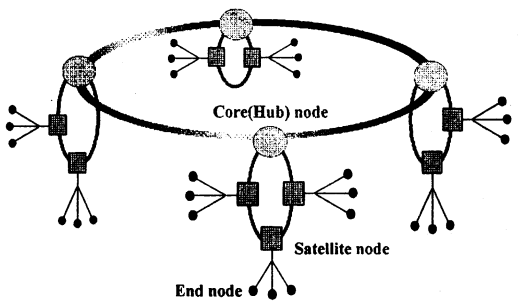

Fig. 1 Typical WDM network for metro areas

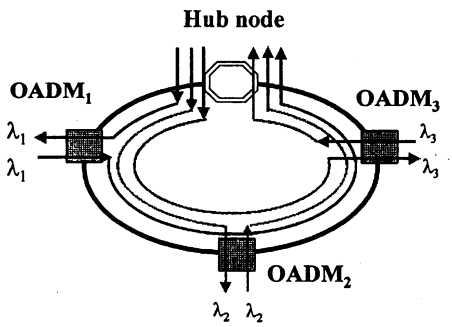

Fig. 2 Basic element of core networks using optical add/drop multiplexers

So far, single- and double-RB have been studied in optical fiber systems. The impact of double RB on digital and analogue fiber systems was precisely analyzed. The basic properties of single RB that gives more penalties than double RB were also studied. However, polarization effects of RB noise were not properly considered. Only a single span without optical amplification and optical sources without modulation were assumed. In this paper we consider single RB in optically amplified multiple spans as well as an optical modulation.

2. The multifiber WDM express network architecture (MWEN)

2.1 Outline

Figure 3(a) shows an example of ring-type MWEN configuration. In this example, there are three nodes (n_1, n_2 and n_3) and three unidirectional fibers. The fibers are terminated at the nodes. In other words, a fiber is dedicated to a designated node. We see that the network is symmetric and can be decomposed into three identical subsystems, one of which is shown in Fig. 3(b). Add/drop operation in the subsystem is as follows: n_2 and n_3 launch wavelengths onto the fiber, which are destined to the n_1. These inserted wavelengths go through intermediate nodes without OEO conversion and segregation, and are finally demultiplexed at the desitnation node n_1. Note that n_2 and n_3 couple to the fiber through optical devices such as optical combiners. Thus, add/drop operation in MWEN's is very simple.

As a consequence, our MWEN architecture offers not only space-division multiplexing, but a number of fiber expressways designated for each nodes. Add/drop multiplexers for MWEN's are very simple, while they allow reconfigurability (i.e., any combination of wavelengths can be inserted at nodes). In Fig. 3, the number of fibers increases as the number of nodes, but a fiber can be shared by several destination nodes in order to reduce the number of fibers. In this case, fiber topology becomes to be helical. In this paper, however, we do not consider the helical topology for the sake of simplicity.

2.2 Design issues

Although MWEN's employ simple OADM's, their WDM efficiency becomes low. Fig. 4, which shows wavelength assignment in Fig. 3, indicates that WDM efficiency of MWEN's becomes as low as 50 %. This is because wavelengths are not reused in MWEN's, whereas they are reused in conventional OADM's as shown in Fig. 2.

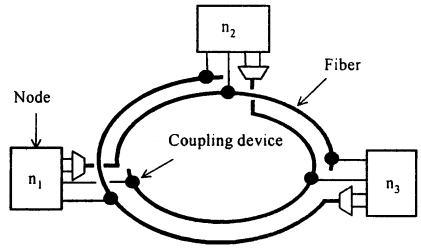

(a) Ring-type network configuration

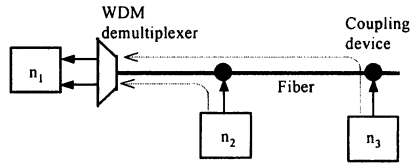

(b) Add/drop operation

Fig.3 Simple example of MWEN's

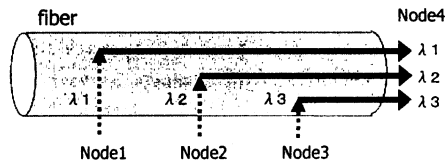

Fig. 4 Wavelength assignment in a unidirectional MWEN

In Fig. 4, we find that wavelengths can also be assigned for left direction because there are open spaces. As a result, we have a new MWEN design using bidirectional transmission shown in Fig. 5. Both ends of a fiber are terminated at two adjacent nodes. This means that two fibers with opposite directions, each of which corresponds to that in Fig. 4, are merged into a single fiber. The two identical sets of wavelengths are assigned for opposite directions except for two different wavelengths that are inserted at both ends. Note that in practical systems a set of consecutive wavelengths (or a wave-band) will be assigned to the nodes 1 to 3 in Fig. 5. We see that wavelengths are reused in Fig. 5, and thus WDM efficiency of nearly 100% can be achieved. As a consequence, the number of fibers necessary in MWEN's can be halved, which makes them more attractive for high-capacity WDM core networks.

In Fig. 5 we see that Rayleigh backscattering (RB) noise can propagate back to an origination node and can interfere with a reverse signal that is launched at the origination node for the opposite direction. The RB noise is an in-band noise, and thus causes a considerable power penalty. In order to reduce the RB noise, we introduce a pair of optical edge filters (EF's) each for both directions at every intermediate node in Fig. 5. For instance, at the node 2, one of the EF's provided for the right direction passes λ0 and λ1 bands, but stops λ2 to λ4 bands because RB noises in the λ2 to λ4 bands will give penalty to reverse λ2 to λ4 bands. The other EF provided for the left direction passes λ3 and λ4 bands, but stops λ0 to λ2 bands for the same reason.

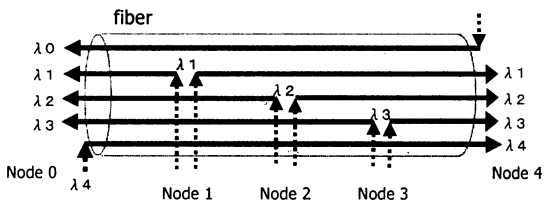

Fig. 5 Bidirectional transmission in an MWEN

The advantage of this idea is that RB noise can be suppressed repeatedly by the EF's, resulting in modest required specifications of them. For instance, the λ1 signal emitted from the node 1 for the right direction will give birth RB noise at every fiber section between two adjacent nodes (i.e., nodes 1 and 2, 2 and 3, and 3 and 4). The RB noise, however, can be reduced by the EF in every node as described above. As a consequence, accumulation of RB noise can be avoided to allow little penalty.

3. Analysis of RB noise in a single span

Our concern is to estimate the effect of RB noise through numerical analysis over multiple amplified spans in the bidirectional MWEN and to show the effect of the EF's. However, let us begin with an analysis of RB noise in a single span, because it gives a basis for the one of multiple spans.

3.1 Basic properties of RB noise

We consider a linearly polarized electrical source field $e(t)$,

$$e(t) = \Re[\varepsilon_s(t)e^{jwt}] \tag{1}$$

with optical frequency w and complex amplitude $\varepsilon_s(t)$, where $\Re[\cdot]$ denotes the real part. $\varepsilon_s(t)$ is given by

$$\varepsilon_s(t) = \sqrt{m(t)}e^{j\phi(t)} \tag{2}$$

where $m(t)$ and $\phi(t)$ denote the complex amplitude terms due to amplitude and phase modulation. The source intensity $I_s(t)$ coupled into the fiber can be expressed as follows.

$$I_s(t) = |e(t)|^2 = m(t) \tag{3}$$

For example, $m(t)$ for IM-DD systems is given by

$$m(t) = \begin{cases} I_m & for\ "1" \\ 0 & for\ "0" \end{cases}$$

$$\overline{m(t)} = I_m/2 = I_a \tag{4}$$

where the overline of $m(t)$ denotes time-average.

For now, we assume that the polarization state is preserved during transmission and backscattering, but we remove this restriction later. Assuming that the source is at z =0, the complex amplitude of the traveling field at location z is then given by

$$\varepsilon(t,z) = \varepsilon_s\left(t - \frac{z}{v}\right)e^{-(\alpha/2 + j\beta)z} \tag{5}$$

where v, α, and β are group velocity, fiber attenuation coefficient, and propagation constant. Since we are mainly interested in a high-speed transmission of Gb/s or more, the relatively slow fluctuation of the optical carrier is not considered here for the sake of simplicity.

The singly Rayleigh backscattered field from a small section of fiber at location z is given by

$$\Delta\varepsilon_{RB}(t,z) = \varepsilon_s\left(t - \frac{z}{v}\right)e^{-(\alpha/2 + j\beta)z}\Delta\rho(z) \tag{6}$$

The reflection coefficient $\Delta\rho(z)$ describes the fraction of backscattered field in relation to the forward traveling field. It has been proved that the polarization state of RB in low birefringent fiber is the same as that of the forward traveling field. We don't have to consider the change of the polarization state at the reflection point. A differential RB coefficient has been defined as

$$\rho(z) = \lim_{\Delta z \to 0} \frac{\Delta\rho(z)}{\Delta z} \tag{7}$$

RB field at the source is given by integrating (6) over the

total fiber length L.

$$\varepsilon_{RB}(t)=\int_0^L \varepsilon_s\left(t-\frac{2z}{v}\right)e^{-(\alpha+j2\beta)z}\rho(z)dz \tag{8}$$

Since the RB signal generated at z traverses from z to the source, the total propagation length from the source becomes to be $2z$ in (8). As a result, the RB intensity at the source is given by

$$I_{RB}(t)=\varepsilon_{RB}(t)\cdot\varepsilon^*_{RB}(t) \tag{9}$$

$$=\int_0^L\int_0^L \varepsilon_s\left(t-\frac{2z_1}{v}\right)\varepsilon^*_s\left(t-\frac{2z_2}{v}\right)e^{-\alpha(z_1+z_2)}e^{-j2\beta(z_2-z_1)} \times\rho(z_1)\rho^*(z_2)dz_1dz_2$$

where * denotes the complex conjugate.

To calculate the time-average of $I_{RB}(t)$, we assume that $\rho(z)$ can be modeled as delta correlated zero-mean circular complex Gaussian (ccG) random variable,

$$\left\langle\rho(z_1)\rho^*(z_2)\right\rangle=2\sigma^2\delta(z_1-z_2) \tag{10}$$

where <x> denotes the expected value (or ensemble average) of x. This assumption has been justified by the fact that the variation of electric fields due to polarization state change, phase noise, and fiber attenuation are extremely coarse compared with the correlation distance of refractive index fluctuations. Note that $\rho(z)$ is a complex function, and σ^2 is the variance of both the real and the imaginary part of $\rho(z)$. Using (10), (9) simplifies to

$$\overline{I_{RB}(t)}=2\sigma^2\,\overline{I_s(t)}\int_0^L e^{-2\alpha z}dz$$

$$=\frac{\sigma^2 I_a}{\alpha}\left(1-e^{-2\alpha L}\right) \tag{11}$$

Comparing (11) with the result for the incoherent case yields

$$\alpha_R S=2\sigma^2 \tag{12}$$

where α_R is the intensity attenuation coefficient due to RB, and S is the fiber recapture factor, which indicates the fraction of the total Rayleigh-scattered power traveling backward in the fiber ($0 \le S \le 1$). As a result, we have a relation between the time-averaged source intensity and the RB intensity with the RB coefficient R_b.

$\overline{I_{RB}(t)}=R_b I_a$, and

$$R_b=\frac{\alpha_R S}{2\alpha}\left(1-e^{-2\alpha L}\right) \tag{13}$$

For example, R_b for standard single-mode fibers is in the range of -35 to -31 dB at 1.55 μm when $L\to\infty$.

3.2 Interference of RB noise and reverse transmission signal

While the time-averaged RB intensity is given by (13), there is another field emitted backward from the source in our model shown in Fig. 5. We assume that the reverse transmission signal has identical signal properties to the original signal. Hence, the total intensity $I(t)$ at the source is

$$I(t)=|\varepsilon(t,0)|^2+|\varepsilon_{RB}(t)|^2 +[\varepsilon(t,0)\varepsilon^*_{RB}(t)+[\varepsilon^*(t,0)\varepsilon_{RB}(t)] \tag{14}$$

The first term in (14) is the reverse signal, the second term is the intensity due to RB, and the third term is their beat noise. The second term is negligible because $|\varepsilon(t,0)|>>|\varepsilon_{RB}(t)|$ holds. Now we have the RB-signal beat noise intensity $I_{RB\text{-}S}(t)$ as follows.

$$I_{RB\text{-}S}(t)=2\Re[\varepsilon(t,0)\cdot\varepsilon^*_{RB}(t)] \tag{15}$$

To find the RB beat noise power spectrum density we introduce the time-averaged autocorrelation function (ACF) of the $I_{RB\text{-}S}(t)$. After some manipulations, we have

$$\overline{R_{RB\text{-}S}}(\tau)=\frac{4}{3}R_b\left(1-e^{-2\alpha L}\right)|R_s(\tau)|^2 \tag{16}$$

The PSD of the RB noise can be obtained by taking the Fourier transform of (16), yielding

$$S_{RB\text{-}S}(f)=\frac{4}{3}R_b\left(1-e^{-2\alpha L}\right)\Im\left\{R_s(\tau)^2\right\} \tag{17}$$

and

$$\sigma^2_{RB\text{-}S}=\int_{-\infty}^{\infty}|H(f)|^2 S_{RB\text{-}S}(f)df \tag{18}$$

where $H(f)$ is the detector frequency response.

3.3 Probability density function of the RB noise amplitude

The RB field is the sum of a large number of reflection components as shown in (7). Since the reflections can be seen to be independent to each other, we assume that the accumulated RB has a Gaussian property (viz., central limiting theory). Actually the RB occurs mainly at the fiber end near the source. Thus, the probability density functions (PDF) of the RB intensity can be approximated

as a gamma function.

$$P_{RB}(i) \approx \frac{i^a e^{-i/b}}{b^{a+1}\Gamma(a+1)} \quad \text{for } i \geq 0 \tag{19}$$

The parameters are given by

$$a = I_b^2/\sigma_{RB}^2 - 1 \text{ , and } b = \sigma_{RB}^2/I_b \tag{20}$$

where I_b is the mean value of RB intensity,

$$I_b = \overline{I_{RB}(t)} = R_b \overline{I_s(t)} = R_b I_a \tag{21}$$

and

$$\sigma_{RB}^2 = \int_{-\infty}^{\infty} |H(f)|^2 S_{RB}(f) df - I_b^2 \tag{22}$$

where $S_{RB}(f)$ is the PSD of the RB intensity. Using the same process as in (16) and (17), and taking the DOP of the RB noise into consideration, $S_{RB}(f)$ is given by

$$\begin{aligned} S_{RB}(f) &= (1+\mathrm{DOP}^2) R_b^2 \, \Im\{R_s(\tau)^2\} \\ &= \frac{10}{9} R_b^2 \, F\{R_s(\tau)^2\} \end{aligned} \tag{23}$$

The reverse signal and the RB noise also interfere and it looks like a multi-path fading channel in wireless communications systems. Thus, the PDF of the total intensity can be approximated by Nakagami-Rice distribution as

$$P_{RB-S}(i) = \frac{\sqrt{i}}{\sigma_{RB-S}^2} e^{-(i+I_a)\sigma_b^2} I_0\left(\frac{2\sqrt{i \cdot I_a}}{\sigma_{RB-S}^2}\right) \tag{24}$$

where $I_0(\cdot)$ denotes the zero-order modified Bessel function of the first kind.

4. RB noise in optically amplified systems

Figure 6 shows an open cascade model for describing how RB noise accumulates over optically amplified multiple spans in bidirectional MWEN's. We assume that there are N spans of RB noise generation and amplification, EDFA's gain G compensates the total loss of a single span, and EF's rejection of RB noise is D. RB noise is generated in every fiber section between nodes, and is amplified and rejected by EDFA's and EF's. The net gain of RB noise at a node becomes to be $\eta = D/G$. The total PSD of RB-signal beat noise at the origination node, σ_N^2, is then given by

$$\sigma_N^2 = K^2 \frac{G}{D}\left(\frac{1-(G/D)^N}{1-G/D}\right)\sigma_{RB-S}^2 \tag{23}$$

where K denotes the detector sensitivity.

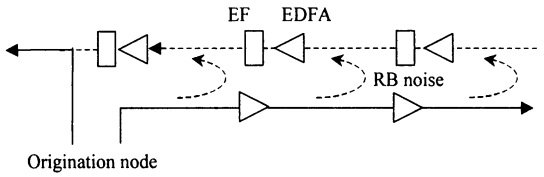

Fig. 6 Cascade model of bidirectional MWEN's

The mean square noise currents for a space and a mark at receiver are given by

$$\begin{aligned} \sigma_{RB,0}^2 &= \sigma_0^2 + \sigma_{RB}^2 \\ \sigma_{RB,1}^2 &= \sigma_1^2 + \sigma_N^2 \end{aligned} \tag{24}$$

where $\sigma_0^2 = \sigma_{sp-sp}^2 + \sigma_n^2$, and $\sigma_1^2 = \sigma_{sp-sp}^2 + \sigma_{s-sp}^2 + \sigma_n^2$.

Finally, the BER is given by

$$BER = \frac{1}{2}\int_0^{\infty} Q\left(\frac{i-i_{th}}{\sigma_1}\right) P_{RB-s}(i)di + \frac{1}{2}\int_0^{\infty} Q\left(\frac{i_{th}-i}{\sigma_0}\right) P_{RB}(i)di \tag{25}$$

The power penalty due to RB noise is given by the increase in signal power required to achieve the same bit error probability (e.g., $BER=10^{-14}$) as that without RB noise.

5. Numerical results

We show several major results due to the space limitations. Fig. 7 shows the effect of the number of spans N on power penalty (PP). We see that PP diverges with N when $\eta < 1$, while it is less than 1 dB when $\eta \geq 1$.The result indicates that RB cannot impede optical transparency when $\eta \geq 1$.

Fig. 8 shows the effect of η on PP over multiple fiber sections. The number of spans N is given in the range of 5 to 15. We see that edge filter rejection should be larger than optical amplifier gain in order to keep PP small.

In Figs. 7 and 8, we see that there are allowable maximum number of spans N_{max} for a given η. Fig. 9 shows the N_{max} in relation to $1/\eta$. We see that η should be greater than 1 in order to apply MWEN's for multiple amplified spans.

As a result, the rejection of edge filters should be

greater than the gain of optical amplifiers. For example, a 40-km fiber span requires 10-dB optical amplifier gain to compensate the fiber loss. In this case, a 10-dB rejection of edge filters is necessary, but it is a moderate requirement.

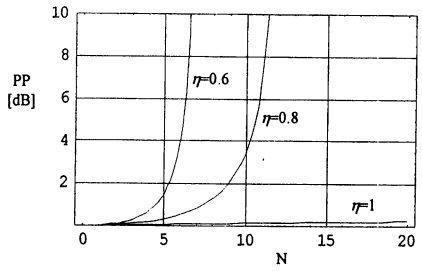

Fig. 7 Power penalty *vs.* the number of spans

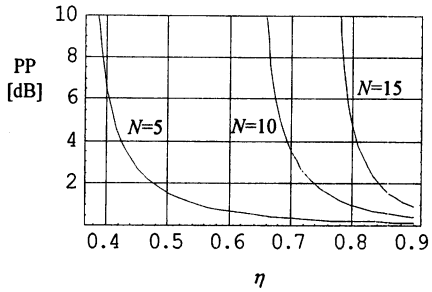

Fig. 8 The number of spans *vs.* η

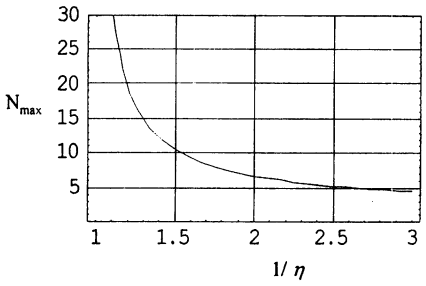

Fig. 9 Allowable maximum number of spans *vs.* $1/\eta$

6. Conclusion

Although the multifiber WDM express network architecture has advantage of simple network design, it has a drawback of relatively low WDM efficiency. We addressed that a new bidirectional design can improve the WDM efficiency as high as 100%. Our numerical analysis showed that the bidirectional design has an optical power penalty due to Rayleigh backscattering, but can be reduced less than 1 dB with simple edge filters of modest rejection (e.g., 10 dB), even though two identical sets of wavelengths are used for opposite directions on a single fiber. We believe that there has been no feasible bidirectional design using two identical sets of wavelengths ever before. Finally, we'd like to stress that the results make multifiber WDM express networks more attractive design option for high-capacity WDM networks.

Acknowledgments

This work was supported by the JSPS under grant No. 17560327.

References

[1] H. Obara, H. Masuda, K. Suzuki, and K. Aida, "Multifiber wavelength-division multiplexed ring network architecture for Tera-bits/s throughput," Proc. of Int. Conf. on Communications, Atlanta, pp. 921-925, 1998.

[2] H. Obara, "Architectural performance analysis of linear-lightwave multifiber WDM networks in grid topology," Electron. Lett., Vol. 36, No. 20, pp. 1720-1722, 2000.

[3] H. Obara and K. Aida "Helical WDM ring network architecture," Electron. Lett., vol. 35, no. 1, pp. 1-2, 1999.

[4] H. Obara, "Cumulative wavelength insertion technique for reducing four-wave mixing noise in multifiber linear-lightwave WDM ring networks," Trans. IEICE, vol. E86B, no. 9, pp. 2835-2837, 2003..

[5] J. Ko, S. Kim, S. Won, and J. Jeong, "Estimation of performance degradation of bidirectional WDM transmission systems due to Rayleigh backscattering and ASE noises using numerical and analytical models," J. of Lightwave Tech., vol. 21, no. 4, pp. 938-946, 2003

[6] H. Obara and M. Sakata, "Novel design of bdirectional WDM ad/Drop rng ntworks esilient to cherent Rayleigh backscattering noise," OECC/COIN, Yokohama, 2004

[7] R. K. Staubli and P. Gysel, "Crosstalk penalties due to coherent Rayleigh noise in bidirectional optical communication systems," J. of Lightwave Tech., vol. 9, no. 3, pp. 375-380, 1991

[8] P.Wan and J. Conradi, "Impact of double Rayleigh backscatter noise on digital and analog fiber systems," J. Lightwave Technology, vol. 14, no. 3, pp. 288-297, 1996

[9] R. K. Staubli and P. Gysel, "Statistical properties of single-mode fiber Rayleigh backscattered intensity and resulting detector current," IEEE Trans. on Communi.., vol. 40, no. 6, pp. 1091-1097, 1992

[10] I. T. Lima, A. O. Lima, Y. Sun, H. Jiao, J. Zweck, C. R. Menyuk, and G. M. Carter, "A receiver model for optical fiber communication systems with arbitraily polarized noise," J. Lightwave Technology, vol. 23, no. 3, pp. 1478-1490, 2005

[11] M. O. van Deventer, "Polarization properties of Rayleigh backscattering in single-mode fibers," J. Lightwave Technology, vol. 11, no. 12, pp. 1895-1899, 1993

[12] M. Nazarathy, W. V. Sorin, D. M. Baney, and S. A. Newton, "Spectral analysis of optical mixing measurements," J. Lightwave Technology, vol. 7, no. 7, pp. 1083-1096, 1989

[13] K. Inoue, K. Oda, and H. Toba, "Crosstalk and power penalty due to fiber four-wave mixing in multichannel transmissions," J. Lightwave Technology, vol. 12, no. 8, pp. 1423-1439, 1994